Absorption and scattering of radiation by a plasma produced by ruby-laser picosecond pulses

V. V. Blazhenkov, A. N. Kirkin, A. V. Kononov, L. P. Kotenko, A. M. Leontovich, G. I. Merzon, and A. M. Mozharovskiĭ

P. N. Lebedev Physics Institute, USSR Academy of Sciences
(Submitted 8 July 1980)
Zh. Eksp. Teor. Fiz. **80**, 144–160 (January 1981)

The angular distribution and the spectrum of the emission scattered by a plasma produced by ruby-laser pulses of ~20 psec duration at a flux density 10^{13}–5×10^{14} W/cm^2 are investigated. It is shown that the absorption coefficient equals 80±10%. The scattered radiation is the result mainly of reflection from the critical surface. The fraction of the stimulated Brillouin scattering in the total energy balance is small. The energies of the scattered optical radiation as well as of the x rays were measured with a time resolution corresponding to the axial period of the picosecond-pulse train. The spectrum, the spatial and angular distributions, and the polarization of the continuous x radiation of the laser plasma are investigated. It is shown that the principal anomalous absorption mechanism responsible for the formation of superthermal electrons is resonant absorption.

PACS numbers: 52.25.Ps, 52.50.Jm

A number of investigations of the physical processes that take place when intense laser radiation interacts with a plasma have been reported in the last few years.[1-6] Particular attention has been paid to investigations of the mechanisms whereby radiation is absorbed by a laser plasma, since knowledge of these mechanisms is of decisive importance for research into laser-mediated controlled thermonuclear fusion. A number of procedures have been developed for the investigation of the absorption processes and for the determination of the principal plasma parameters, such as the electron density, temperature, and others. These procedures include high-speed interferometry,[7] investigation of the spectral composition of the radiation scattered by a plasma,[4,8,9] x-rays emitted by the plasma,[10] the fast particles produced in the plasma,[11] and others.

We have experimentally investigated the optical and x-ray emission from a plasma produced by picosecond pulses of a ruby laser in the flux-density range 10^{13}–5×10^{14} W/cm^2. The results were used to calculate the plasma parameters and to determine the basic mechanism of the absorption of the laser emission.

EXPERIMENTAL SETUP

We used a mode-locked ruby laser at low temperature (100 K). The laser construction is described in detail in Ref. 12. It generated a short train of 1–3 pulses with minimum duration 10–20 psec and with a total energy up to 0.5 J. The interval between pulses, with the exception of specially stipulated cases, was 4 nsec. The radiation was linearly polarized with a degree of polarization not worse than 0.9. The laser beam was focused with a lens of $f=50$ mm into a spot of 60 μm diameter at half-intensity. The maximum radiation flux density at the target reached 5×10^{14} W/cm^2. We used bulky targets of different materials with atomic number from 6 to 74. The targets were placed in a vacuum chamber evacuated to a pressure 10^{-3} Torr. The x-ray detectors were insulated from the chamber, but the target holder was in contact with the chamber housing.

The experimental data were accumulated and reduced with a multichannel automatized facility with on-line CAMAC, NIM, and minicomputer electronic modules.[13] The signals from the x-ray detectors were converted into a digital code by an AD-811 11-digit amplitude-digital converter,[14] while the signals from the coaxial photocells that measured the energy of the laser radiation were digitalized with a charge-digital QD-808 converter.[14] The experimental data were recorded on a floppy disk and printed on a teletype. The graphic information was reproduced by a Tektronix-613 display and an NE-230 plotter.

OPTICAL RADIATION SCATTERED BY PLASMA

The optical radiation scattered (reflected) by a laser plasma is an important factor in the plasma diagnostics.[1,2,9] The angular distribution of this radiation characterizes the shape of the critical surface and makes it possible to assess the mechanisms of the scattering of the radiation. Its spectral composition yields information on the mechanisms of laser-energy absorption, on the rate of plasma expansion, on the plasma electron temperature, and others. We have investigated the angular and spectral distribution of the radiation scattered by the plasma, and determined the absorption coefficient and the character of its variation along the path of the pulses.

TABLE I. Dependence of the degree of polarization (in %) of the x rays on the observation direction, on the target material, and on the incidence angle.

Target material	Position 1			Position 2
	0°	15°	35°	0°
C	10	9	–	3
Al	14	14	–	–
Cu	7.5	11	–	–
Mo	12.5	12	–	11
W	12	13	8.5	12

 0038-5646/81/010072-09$02.40

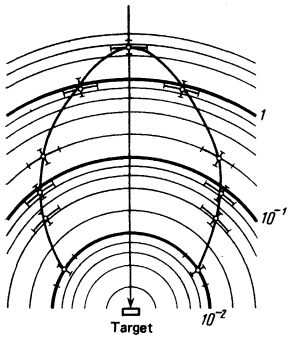

FIG. 1. Directivity pattern of the scattered radiation for the case of normal incidence on a copper target. Pulse duration $\tau \approx 10-100$ psec, radiation flux density $I \approx 10^{13}-10^{14}$ W/cm^2.

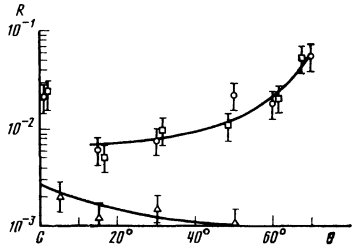

FIG. 2. Specular reflection coefficient for p-(□) and s-polarization (○) of laser radiation and of the reflection into the aperture of the focusing lens (△) on the angle of incidence on an aluminum target, $\tau \approx 10-100$ psec, $I \approx 10^{13}-10^{14}$ W/cm^2.

1. Angular distribution of the scattered radiation

The angular distribution of the radiation scattered by the plasma was investigated at various incidence angles with the aid of energy-calibrated FK-19 photocells. The measurements were made in a plane perpendicular to the vector of the electric field of the heating radiation. The maximum radiation intensity in these experiments was ~10^{14} W/cm^2. We used targets made of various materials ranging from carbon to tungsten; the results obtained with all targets were similar within the limits of experimental error.

Figure 1 shows the directivity pattern of the scattered radiation in the case of normal incidence of a laser beam on a copper target. The coefficient of reflection into the aperture of a lens of 14 mm diameter with focal length 50 mm was $2.8 \pm 0.5\%$. The directivity pattern was qualitatively similar to that observed in Ref. 15. The value of the total reflection coefficient of the plasma, obtained by integrating the directivity pattern a solid angle 2π, was $20 \pm 10\%$. This is somewhat less than the values measured in Refs. 2, 16, and 17 at a wavelength 1.06 μm, and corresponds approximately to the values measured in Refs. 17 and 18 and wavelengths 0.53 and 0.26 μm at comparable flux densities and pulse durations.

With the radiation obliquely incident on the target, the directivity pattern reveals a maximum corresponding to specular reflection. This is evidence that the spreading of the plasma over a scale on the order of the focusing-spot radius is on the whole planar, i.e., the deviations of the critical surface from a plane are much less than the dimension of the focusing spot. However, as will be shown later on, small-scale modulation of the critical surface, and its bending on the periphery, are possible. The directivity pattern for inclined incidence had a weak asymmetry. Thus, at an incidence angle 15° the reflection coefficient at an angle −15° (into the aperture of the focusing lens) was 0.2%, and at an angle 45° (symmetrical relative to the specular maximum) only 0.05%. This can attest to the appearance of stimulated Mandel'shtm-Brillouin scattering (SMBS) in the laser-plasma corona.

Figure 2 shows the dependence of the coefficient of specular reflection on the angle of incidence on an aluminum target for p- and s-polarization of the laser radiation and for reflection into the aperture of the focusing lens. The general appearance of the curves is similar to that obtained in Ref. 16, but the absolute values of the reflection coefficient are smaller in our case. The relations between the scattering, due to SMBS, into the aperture of the focusing lens and the specular reflection from the critical surface are also different. In Ref. 16 the contributions of the SMBS and of the specular reflection are approximately equal. In our case, at a radiation flux density smaller by a factor of 10, the SMBS makes a smaller contribution than the specular reflection. In contrast to Refs. 17–19, we did not observe, within the limits of the measurement accuracy, a difference between the specular reflection coefficients for the p- and s-polarization at comparable flux densities. This is possibly due to the already mentioned small-scale modulation of the critical surface. The increase of the reflection coefficient at incidence angles larger than 60° agrees with the results of Ref. 16 and may be evidence that the plasma electron density N_e undergoes an abrupt change in the region between N_{cr} and $\frac{1}{4}N_{cr}$.

The absorption coefficient $80 \pm 10\%$ measured by us greatly exceeds the estimate based on an inverse bremsstrahlung mechanism for a pulse of 20 psec duration at a plasma electron temperature $T_e \approx 0.5-1.0$ keV.[6] This indicates that the anomalous absorption mechanisms make a noticeable contribution, comparable with the inverse bremsstrahlung, to the total energy balance.

2. Time dependence of reflection

Since no single ultrashort pulse was separated in our experiments, the conditions of absorption of the laser radiation by the plasma could, strictly speaking, vary from pulse to pulse. We have therefore measured to coefficient of reflection into the aperture of the focusing lens with a time resolution corresponding to the spacing of the train pulses. The signal from the photocell that recorded the scattered radiation was fed through a cable delay line to an I2-7 oscilloscope, which received also a signal from the photocell that recorded the radiation incident on the target. The time resolution of the recording system was ~1.0 nsec. The amplitudes of the pulses on the oscillograms were proportional to the energies of the corresponding light pulses. A statistical reduction of ~100 oscillograms has shown that, on the average, the reflection coeffi-

cient is constant over the train of the ultrashort pulses. This indicates that the plasma produced by the first pulse of the train manages to become dispersed during the time between two pulses. This does not mean, however, that the radiation is absorbed under identical conditions (i.e., on the same plasma-density profile) for all the pulses of the train.

3. Spectral composition of the scattered radiation

In addition to the measurements of the energy of the plasma-scattered radiation, we investigated its spectral compositions. The measurements were made at normal incidence on bulky flat targets of carbon, copper, and tungsten. The spectral width of the laser radiation was ~1 cm^{-1} (~0.5 Å). We investigated the spectrum near the laser frequency ω_0 as well as near the frequencies $2\omega_0$ and $(\frac{3}{2})\omega_0$. An STÉ-1 spectrograph was used (dispersion for ω_0 in third-order diffraction was ≈13 Å/mm). The distance between the spectrograph and the target was 3 m. We registered radiation scattered into the aperture of a focusing lens of 20 mm diameter and focal length 50 mm.

The spectra of the scattered radiation near ω_0 were registered for a single laser flash. Typical spectra and the corresponding density distributions are shown in Fig. 3. In all the laser flashes and on all the targets the spectrum of the scattered radiation near the fundamental frequency was broader than the spectrum of the heating radiation, and reached 12 Å in width. The center of gravity of the spectral distribution was shifted to the long-wave side by 1–3 Å in the case of the carbon target, 3–6 Å for copper, and 4–8 Å for tungsten. The short-wave end of the spectrum for the tungsten target was located on the average 3 Å away from the laser-radiation wavelength λ_0. In the case of the copper target, the short-wave end was near λ_0, while for the carbon target it was shifted towards the blue region by a value −4 Å [Fig. 3(a)]. In a number of flashes, oscillations of the intensity were observed in the spectrum of the scattered radiation [Fig. 3(b)],

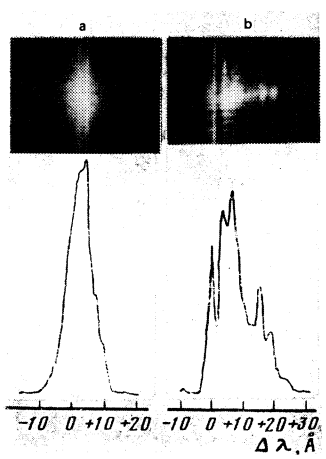

FIG. 3. Spectrogram of radiation scattered into the aperture of the focusing lens at normal incidence on the target, obtained near the laser-radiation wavelength λ_0 (top) and the corresponding density distributions (bottom): a—carbon target, b—tungsten target.

with a period 3–5 Å. This modulation occurred almost always when strong superthermal x rays were present.

The plasma radiation at the $2\omega_0$ harmonic and near the frequency $\frac{3}{2}\omega_0$ could not be registered even when the exposure was lengthened to ~50 flashes. An estimate of the $2\omega_0$ radiation intensity yields $I_{2\omega_0} < 10^{-3} I_{\omega_0}$, where I_{ω_0} is the intensity of the scattered radiation at the fundamental frequency.

The results agree with the measurements of the spectrum of the scattered radiation near the fundamental frequency, performed in Refs. 8 and 9. The spectral composition of the radiation near ω_0 is determined by the joint action of two mechanisms: SMBS in the corona of the laser plasma, and the Doppler effect produced by scattering in the dispersing plasma. As shown in Ref. 8, the plasma region that moves with subsonic velocity gives a red shift, while the tenuous-plasma region with supersonic dispersal velocity can give a blue shift. The blue shift registered by us in the case of the carbon target, and its absence when copper and tungsten targets were used, agree with the experimental results of Ref. 9, where it was observed that the threshold flux density at which the blue shift takes place increased with increasing atomic number of the target material. This quantity amounted to $(2-3)\times 10^{13}$ W/cm^2 for $(CH_2)_n$ at a pulse duration ~5 nsec. The appearance of the oscillations of the spectral intensity is likewise in good agreement with the results of Ref. 4, where the spectrum observed had a line structure with a period 1–2 Å at $I \gtrsim 10^{14}$ W/cm^2.

Thus, under the conditions of our experiment, SMBS takes place in the laser-plasma corona. This process, however, makes a small contribution to the reflection coefficient. This is attested to by the character of the angular distribution of the scattered radiation, by the low value of the reflection coefficient, and by the fact that it does not vary along the train.

From the position $\delta\lambda_b$ of the blue boundary of the spectrum we can estimate the rate of dispersal u of a cold tenuous plasma in which SMBS sets in:

$$u \approx \left(1-\frac{c\delta\lambda_b}{2c_{ac}\lambda_0}\right)c_{ac} \approx 1.5\, c_{ac},$$

$c_{ac} \approx 1.5\times 10^7$ cm/sec at $T_e \approx 400$ eV for carbon.

In addition, we can estimate the speed of sound in the plasma region where most of the light scattering takes place. From the expression for the wavelength of the scattered radiation

$$\Delta\lambda = \frac{2\lambda_0}{c}(c_{ac}-u)\left(1-\frac{N_e}{N_{cr}}\right)^{1/2}$$

we obtain $c_{ac} \gtrsim c\Delta\lambda/2\lambda_0$. Since $\Delta\lambda \approx 5$–15 Å, we have $c_{ac} \gtrsim (1-3)\times 10^7$ cm/sec.

INVESTIGATION OF THE PLASMA X RADIATION

The x rays from a laser plasma serve as one of the most important sources of information on the processes in the plasma. They are characteristics of the plasma electron temperature and of the electron velocity distribution, and help identify the mechanisms of laser-radiation absorption and of the appearance of super-

thermal electrons. In the present study we investigated the spectrum and the angular and spatial distributions of the continuous x radiation from a laser plasma.

1. Pinpoint photographs of a laser plasma

The spatial distribution of the x radiation of a laser plasma in the 1–3 keV range was investigated by taking pinpoint photographs of the x radiation. They were taken on UF-VR photographic film through a diaphragm perpendicular to the target plane and having an 8 μm diameter hole. A copper target was used. The spectral range of the registered radiation was determined by the thickness of the beryllium filter placed in front of the photographic film. Pinpoint photographs obtained at various filter thicknesses are shown in Fig. 4(a). Figure 4(b) shows the density distributions of the flare, taken through a filter 48 mg/cm^2 thick (cutoff energy $E_c = 3$ keV). It is seen that the luminous region decreases with increasing filter thickness. For the very thinnest filter the flare dimension along the normal to the target was ~100 μm, and the total dispersal angle was 25°. For the thickest filter, the thickness of the luminous region on the pinpoint photograph was closest to the smallest attainable in the given geometry and equaled 20 μm. This minimum dimension was determined by the resolution of the pinpoint camera, which in this case was equal to the diaphragm diameter,[20] and by the distance from the center of the diaphragm to the plane of the target (0.7 mm). Consequently the dimension of the region occupied by the dense hot plasma should be much smaller than this dimension. We note that the dimension of the plasma flare on the pinpoint photographs obtained in Ref. 1 using pulses of nanosecond duration was much larger, at comparable beryllium filter thicknesses, than in our case.

The size of the luminous region of the plasma in the target plane depends little on the filter thickness and corresponded to the diameter of the focusing spot on the target surface. This means that there is no substantial transfer of plasma energy in the radial direction via heat conduction or via dispersal over the target surface after the termination of the laser pulse. The size determined from the pinpoint photographs agrees also with the estimate based on the width, measured by us earlier,[21] of the spectral lines of multiply charged ions.

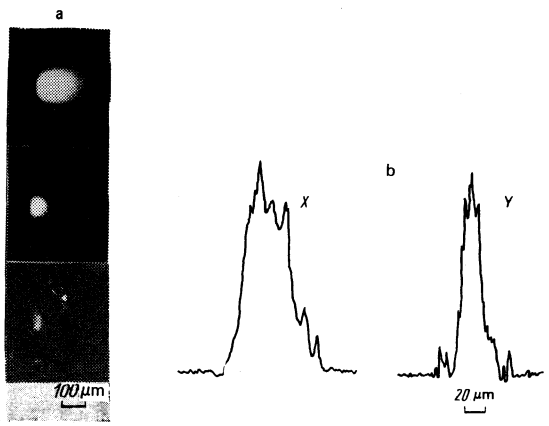

FIG. 4. a) Pinpoint photograph of plasma flare, taken through beryllium filters of thickness 16 mg/cm^2 (top), 32 mg/cm^2 (middle), and 48 mg/cm^2 (bottom). b) Density distribution of flare, taken through a filter 48mg/cm^2 thick, X—in the target plane, Y—perpendicular to the target plane.

2. Spectrum of continuous x radiation

The experimentally simplest and most widely used method of measuring the spectra of continuous x radiation is the wide-band filter method,[22] in which one registers the absorption curves of the investigated x radiation as it passes through filters with different thicknesses. To find the differential spectrum (i.e., the spectral density of the radiation) from the absorption curve obtained in this manner, one uses numerical reconstruction methods based usually on the regularization method.[23] In this reconstruction method, however, it is difficult to estimate the errors of the results, since quite complete information on the spectrum must be on hand before a correct solution is obtained.

The form of the response function of the detector can be substantially improved, and the reduction and accuracy of the measurement of the x-ray spectra simplified thereby, by using the Ross-filter (K-filter) procedure,[24] which consists of measuring the x rays in discrete subbands of the energy band determined by absorption K-band of the employed filter. This method was proposed for the investigation of a laser plasma in Ref. 25. Since the spectrum of the continuous x radiation from a laser plasma falls off strongly with increasing photon energy, these measurements are usually performed with a Ross spectrometer that contains one filter and one x-ray detector, rather than the two used in the classical Ross spectrometer.

The x-ray spectrum was investigated by us earlier with the aid of wideband aluminum filters.[6] In the present study we investigated the differential x-ray spectra with a spectrometer containing K-filters and scintillation counters based on CsI(Tl) crystals, with FÉU-85 photomultipliers, in front of which we placed filters of Ti (150 μm), Fe (100 μm), Co (120 μm), Cu (150μm), Zn (120 μm), Zr (300 μm), Mo (300 μm), Cd (600 μm), and $BaTiO_3$ (1000 μm). The spectrometers operated in the energy band from 5 to 37 keV. The recording system accommodated a dynamic range of 4–5 orders. This range was reached by using AD-811 analog-digital converters and by suitable selection of the K-filter thickness and of the diameters of the holes in the lead collimators in front of the filters. The spectrometers were energy-calibrated automatically using the radioactive γ isotopes ^{55}Fe (5.9 keV), ^{109}Cd (22.5 and 88 keV), and ^{22}Na (511 and 1280 keV).

Figure 5 shows the differential spectra of the x rays from a tungsten plasma, obtained with the aid of K-filters in various series of flashes. Each curve was obtained by averaging over ~10 flashes with close values of the x-ray energy. The form of the spectrum corresponds to a two-temperature distribution with an electron temperature T_e and with an effective superthermal-electron temperature T_s. The inflection point of the spectral distribution lies in the 8-keV re-

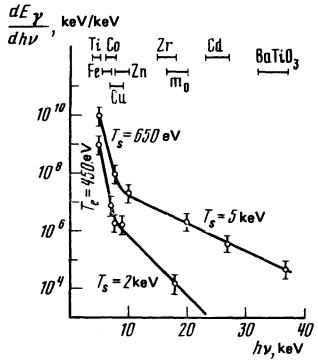

FIG. 5. Differential specturm of x rays from tungsten plasma in two laser-flash runs. On the horizontal axis are marked the width of the pass bands of the K-filters at the 0.1 level.

gion and separates the sections with predominant thermal radiation (recombination radiation of thermal electrons) and superthermal radiation (bremsstrahlung of superthermal electrons). The obtained values of T_e and T_s agree well with the values obtained by us with wide-band filters. The form of the x-ray spectrum agrees with the data obtained in Refs. 3 and 26 at approximately the same laser-radiation flux densities.

Figure 6 shows a plot of T_s against T_e, obtained from differential x-ray spectra similar to those shown in Fig. 5. This dependence can be approximated by the expression $T_s \propto T_e^2$.

3. Influence of prepulse on the x-ray output

It is known that the prepulse influences the interaction of the radiation with the laser plasma, since it determines to a considerable degree the electron-density profile with which the main pulse interacts. As shown in Ref. 27, the intensity and spectrum of the plasma x rays depend substantially on the prepulse. We have therefore measured the x-ray energy of the plasma produced by each laser pulse in the train.

We used for the registration a detector consisting of a plastic scintillator (p-terphenyl in polystyrene) and an FÉU-87 photomultiplier. The time resolution at half-amplitude was 4 nsec. The energy resolution of the detector was 15% for the 662-keV line of ^{137}Cs. The detector signal was fed to an I2-7 oscilloscope. The same oscilloscope input received a signal from a photocell that registered the laser radiation. The photomultiplier signal was delayed ~15 nsec relative to the FK-19 signal. The axial period of the resonator was in this case 7 nsec. The x rays were registered in two spectral regions that were set by the thickness of the aluminum absorber placed ahead of the x-ray detector. We used absorbers with cutoff energies 5 and 12 keV. These spectral ranges corresponded to the thermal and superthermal radiation.

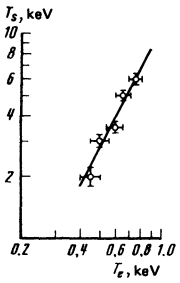

FIG. 6. Dependence of effective temperature T_s of the superthermal electrons on the plasma electron temperataure T_e for a tungsten target.

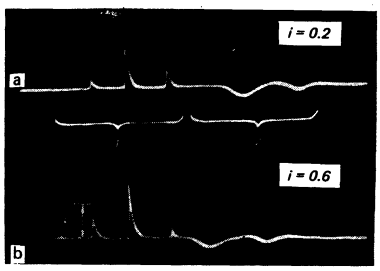

FIG. 7. Oscillograms of plasma x rays at various prepulse amplitudes i; E_e = 12 keV, 1—laser radiation, 2—x radiation.

Typical oscillograms for a cutoff energy 12 keV are shown in Fig. 7. The relative amplitude i of the prepulse ahead of the maximum-amplitude pulse ranged from 0.1 to 1.0 and usually amounted to 0.2. The total background energy did not exceed ~10^{-3} of the energy of the ultrashort pulses. The form of the x-ray pulse train depended on the prepulse amplitude. At i = 0.1–0.4 the maximum x-ray pulse corresponded as a rule to the maximum laser pulse [Fig. 7(a)]. At large values of i, the probability that the maximum x-ray pulse was produced by the main pulse decreased [Fig. 7(b)]. The dependence of this probability W on i for the cutoff energy 12 keV is shown in Fig. 8. A similar dependence was obtained also for the cutoff energy 5 keV.

As shown by measurements of the reflection coefficient with the time resolution corresponding to the train period, the x-ray absorption was the same for all the train pulses. At the same time, the conversion of laser radiation into x rays with photon energy ~5 keV is more effective in the prepulse than in the main pulse of the train. This can be attributed to the following factors. During the interval between the prepulse and the main pulse, the plasma produced by the prepulse becomes dispersed. Therefore the main pulse passes on its way to the target through a layer of tenuous and relatively cold plasma, which can have an appreciable optical thickness. Thus, the electron temperature averaged over space and the degree of ionization of the

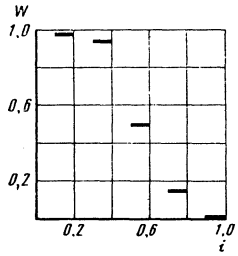

FIG. 8. Probability W that the maximum of the x radiation corresponds to the main laser pulse vs. the amplitude of the prepulse i; E_e = 12 keV.

plasma produced by the main pulse will be lower than in the case of the prepulse, if the latter is of considerable amplitude. The recombination-radiation spectrum is shifted to the softer region and its intensity in the $E_c = 5$ keV region decreases.

The character of the laser-radiation absorption in the critical region is also different for the prepulse and the main pulse. The fraction of the radiation reaching the critical region of the plasma decreases in the presence of a strong prepulse. In addition, the main pulse acts on a smoothed electron-density profile, and this creates unfavorable conditions for the resonant absorption that takes place near the critical region of the plasma. At the same time, as will be shown below, the resonant absorption is the principal mechanism for the formation of superthermal electrons under our conditions. Therefore the x rays in the region of $E_c = 12$ keV, which constitute bremsstrahlung of superthermal electrons, become weaker for the main pulse when the prepulse amplitude is increased.

4. Dependence of effective temperature T_s of superthermal electrons on the laser-radiation flux density

When measuring the dependence of T_s on the laser-radiation flux density, the latter was calculated with account taken of the energy distribution in the focal spot and of the duration and of the number of pulses in the train. Laser pulse durations in the interval from 200 to 40 psec were measured by an electron-optical camera, and in the interval from 50 to 10 psec by a high-speed optical shutter and saturating filter.[28]

The measured $T_s(I)$ plots are shown in Fig. 9. The plot has the $I^{1/2}$ for typical resonant absorption[29] at not too high radiation flux densities, before the electron density profile deformation sets in. The absolute values of T_s exceed somewhat the results of the theoretical calculations,[29,30] but are close to recent experimental results.[2,26,31-34] It should be noted that the values of T_s at the same flux density but at different pulse energies and durations were equal within the limits of experimental error.

In contrast to Ref. 34, where the superthermal radiation (in the case of pulses of 3.5 nsec duration at I up to 2×10^{14} W/cm^2) was observed only at incidence angles $\leq 45°$, we have observed this radiation at incident angles up to 70°. The possibility of the onset of absorption mechanisms under this condition may be related to local perturbations of the critical surface.

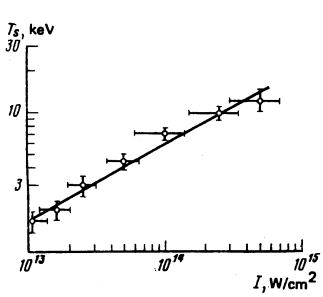

FIG. 9. Effective superthermal-electron temperature T_s vs. the laser-radiation flux density I for a copper target.

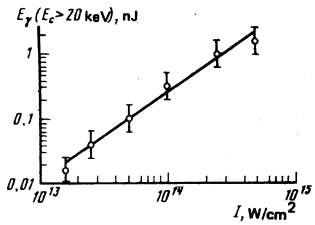

FIG. 10. Dependence of energy E_s of superthermal x radiation passing through an aluminum filter with cutoff energy 20 keV on the laser-radiation flux density on a copper target. Laser radiation energy at target 0.2 J.

We performed simultaneously absolute measurements of the energy of the superthermal x radiation as a function of the laser-radiation flux density. The measurement results for a cutoff energy $E_c = 20$ keV (at a laser radiation energy 0.2 J at the target) are shown in Fig. 10.

5. Measurement of the angular distribution

The angular distribution of the continous x radiation yields information on the isotropy of the plasma-electron distribution. In particular, the angular distribution of the x-ray bremsstrahlung is sensitive to the mechanisms of superthermal-electron production. As shown in Ref. 35, in the case when the electrons have preferred directions of motion, the angular distribution of the bremsstrahlung has a minimum in this direction. Observation of the anisotropy of the x rays with a minimum in the direction of the vector **E** has led the authors of Ref. 36 to the conclusion that parametric instabilities develop in this case.

We have measured the angular distribution of the continuous x radiation in a wide spectral range, using targets of different materials with atomic numbers from 13 to 74. The measurements were made both in the target plane and in the laser-radiation polarization plane.

In the cutoff-energy region from 2 to 5 keV the x rays were registered on UF-VR photographic film. The measurements have shown that the angular distribution is isotropic in both investigated accurate to ±10%. For the measurements in the cutoff-energy range from 12 to 25 keV we used up to 32 scintillation detectors arranged on a sphere with the target at its center.

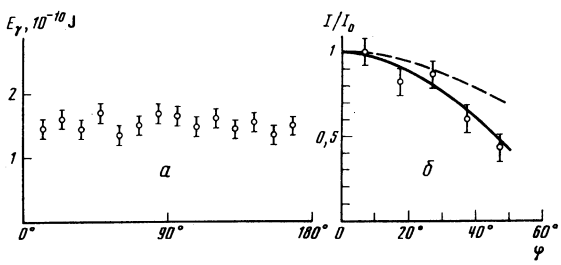

FIG. 11. Angular distribution of continuous x radiation for a copper target at $I \sim 10^{14}$ W/cm^2 at a cutoff energy 16 keV. a) in the target plane, b) in the laser-beam polarization plane.

The measurement results for a copper target at a flux density ~10^{14} W/cm^2 and aluminum-target cutoff energy 16 keV are shown in Fig. 11. The dashed line in Fig. 11(b) marks the results calculated with allowance for the vacuum-chamber wall thickness. The isotropy of the angular distribution in the target plane and the anisotropy in the polarization plane point to the presence of a flux of superthermal electrons in the plasma near the normal to the target.

6. Measurement of the polarization of superthermal x radiation

The polarization of bremsstrahlung x rays, as well as their angular distribution, is sensitive to the directions of the electron fluxes in the plasma. Thus, for example, the polarization of the solar-corona x radiation has revealed the presence of electron fluxes in the corona. The polarization of the x radiation of a laser plasma was first observed by Godwin *et al.*[37] and investigated in Refs. 38 and 39.

To measure the degree of polarization of the continuous x radiation we used a Thomson polarimeter consisting of an LiD scatterer and two pairs of mutually perpendicular scintillation counters based on NaI(Tl) with dimensions 30×30 mm and FÉU-85 photomultipliers (Fig. 12). One more spectrometer was placed behind the scatterer and served to monitor the x-ray energy passing through it. The spectrometers placed on the target chamber were used to determine the effective temperature T_s of the superthermal electrons. The exit window of the vacuum chamber was sealed with aluminum foil 100 μm thick. The accumulation of the data from the polarimeter spectrometer and the calibration of the spectrometer channels were automatic. For the calibration we used the radioactive γ isotopes ^{55}Fe (5.9 keV) and ^{109}Cd (22.5 and 88 keV). The drift of the position of the photopeak of the calibration isotope during the two-hour measurement run did not exceed ±1%. To exclude systematic measurements, the spectrometer pairs changed places after each measurement run.

The lower x-ray photon-energy limit registered by the polarimeter spectrometers was ~12 keV. It was determined only by the thickness of the exit window of the vacuum chamber (100 μm of Al) and by the scatterer material LiD. For the scatterer used in the study,

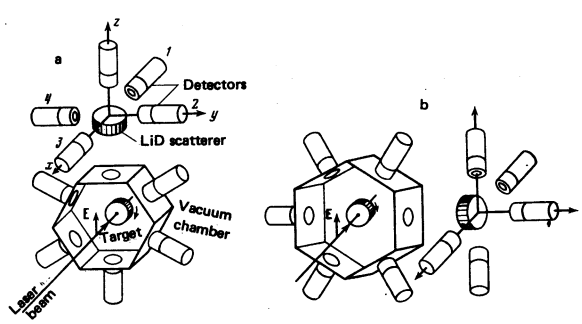

FIG. 12. Setup for the measurement of the polarization of continuous x radiation. a) position of polarimeter 1, b) position of polarimeter 2.

the cross section of the Compton effect exceeds the cross section of the photoeffect at a photon energy ≳9 keV. As follows from our earlier results[8] and the measurements of the differential spectra, the main contribution to the continuous x radiation in the registered energy region ≳12 keV is made by the superthermal-electron bremsstrahlung.

The polarimeter is mounted in such a way that the collimated x-ray beam from the target is incident on the scatterer in a direction parallel to the vector **E** of the laser radiation [Fig. 12(a)] in one measurement run (position 1). In the other run (position 2) the vacuum chamber and the polarimeter were rotated 90° around the optical axis of the system [Fig. 12(b)]. In position 1 the polarimeter could register the presence in the plasma of an electron flux normal to the target. In position 2 it was possible to register fluxes directed both normal to the target and along the vector **E**.

The experiments were performed on targets of carbon, aluminum, copper, molybdenum and tungsten with atomic numbers Z from 6 to 74. The angle of incidence of the laser beam on the target (p-polarization) ranged from 0 to 35°. Inclination did not change the relative position of the polarimeter and target.

The measurement results are listed in Table I. The values of P (the degree of polarization of the x rays) in the table are given by the expression

$$P=\frac{(E_2+E_4)-(E_1+E_3)}{(E_2+E_4)+(E_1+E_3)},$$

where E_i are the readings of the ith spectrometer.

As seen from the table, observations in position 1 showed polarization of the continuous x radiation for all the investigated targets and incidence angles. The degree of polarization was independent, within the limits of the measurement error (±4%), of the incidence angle and of the target material, and its average value was 12%.

The measurements in polarimeter position 2 were made on targets of carbon, molybdenum, and tungsten at normal incidence. In the case of the molybdenum and tungsten targets the degree of polarization had the same sign and the same absolute value as the degree of polarization measured in position 1. For the carbon target the degree of polarization was less, 3–4%.

The results point to the existence of a flux of superthermal electrons in a direction close to the normal to the target, i.e., of a plasma-density gradient, thus corresponding to resonant absorption. The agreement between the degrees of polarization of the molybdenum and tungsten targets when observed in positions 1 and 2 point to the absence of noticeable electron fluxes in the direction of the vector **E**. The decrease of the degree of polarization in the case of the carbon-target when observed in position 2 is possible due to the onset of a flux of superthermal electrons along the vector **E** as a result of the development of parametric instabilities, which have lower thresholds for lighter-element plasmas. The possible development of parametric instabilities for a carbon plasma at a heating pulse

duration ~10 psec may be due in our case to an increase in the spatial scale of the critical region as a result of the presence of a prepulse.

Comparison of the measured degree of polarization with the results of calculations[35,40] with account taken of the real energy spectrum of the superthermal x rays suggests that the dispersal of the superthermal electrons takes place in a rather wide cone. The apex angle of the cone is estimated at ~60°. This value agrees well with the results of Ref. 11, where the dispersal angles of the superthermal electrons were measured directly. An exact quantitative comparison of the results with the calculations of Refs. 35 and 40 is difficult, since these calculations were made for collimated monochromatic electron beam.

No dependence of the degree of polarization on the laser-beam incidence angle was observed in the experiment, within the limits of the measurement accuracy. This leads to the following conclusions: 1) There are no fluxes of superthermal electrons in directions other than normal to the target. 2) the angular maximum of the resonant absorption is larger than the value that follows formally from the theory,[41] in agreement with the results of Refs. 42 and 43. 3) Fast electrons with isotropic velocity distribution, which produce depolarized bremsstrahlung, constitute a small fraction of the total number of superthermal electrons.

The presence of noticeable resonant absorption at normal incidence on the target seems at first glance to contradict formally the theory of this effect. The possibility of the onset of resonant absorption at normal incidence is apparently due to the difference between the critical surface from a plane because of the small-scale modulation,[44] and also because the dispersal of the plasma is no longer one-dimensional in the peripheral region. In this case the absorption takes place on those sections of the critical surface where the angle between the density gradient and the electric-field vector takes on a value that is optimal for resonant absorption. In this case the direction of the dispersal of the superthermal electrons that are accelerated by resonant absorption should make with the laser-beam axis a nonzero angle close in magnitude to the optimal resonant-absorption angle. This explains possibly the large range of dispersal angles of the superthermal angles.

DISCUSSION OF RESULTS

A comparison of the experimentally obtained laser-radiation absorption coefficient $K=80\pm10\%$ with the theoretical estimates shows that so large an absorption cannot be attributed to inverse bremsstrahlung alone. Indeed, the characteristic electron-density scale L, which determines the value of the absorption coefficient, cannot exceed the quantity $c_{ac}\tau$ (τ is the laser pulse duration), which equals 2–3 μm at $\tau=20$ psec and at $T_e=0.5$–1 keV. As shown by the reduction of the pin-point photography, this quantity is at any rate less than 10 μm. The form of the dependence of the reflection coefficient of the laser radiation on the incident angle indicates that L is apparently even smaller, $L\sim\lambda$.

The fact that the experimentally measured absorption coefficient was independent of the pulse duration is evidence that the characteristic scale depends little on the duration. Therefore $L\leq c_{ae}\tau_{min}$ (τ_{min} is the shortest pulse duration in the experiment), and it can be estimated at ~1 μm. For so small a value of L the absorption coefficient for inverse bremsstrahlung is 20–40% for targets with Z ranging from 6 to 74. Thus, an important role in the energy absorption is played in our case by anomalous absorption mechanisms.

The main contribution to the anomalous absorption under conditions of our experiment is made by the resonance mechanism. This is confirmed by the character of the polarization of the plasma x-ray bremsstrahlung, by the form of its angular distribution, by the character of the dependence of T_s on the flux density, and by the independence of the absorption coefficient of the atomic number of the target material.

At the same time, the measurements have shown that model calculations based on resonant absorption[29] do not explain many significant experimental features, particularly the difference by a factor 2–10 between the measured and calculated T_s, the larger width of the resonant maximum than predicted by the theory, the presence of superthermal electrons at normal incidence of the laser beam, as well as the stronger dependence of T_s on T_e than predicted in Ref. 29. Some of these features can be attributed to the small-scale modulation of the critical surface, which leads to the onset of resonant absorption at normal incidence.

The stronger absorption than obtained in Refs. 16 and 26 with a neodymium laser is apparently due to the large value of N_{cr}, which increases the fraction of the absorbed energy. This agrees well with the result of Ref. 17, where a higher absorption coefficient was observed at the second harmonic of the Nd laser compared with the first harmonic.

The authors thank M. D. Galanin for interest in the work, G. A. Askar'yan and S. D. Zakharov for a discussion of the results, and R. G. Mirzoyan for help with the work.

[1]Yu. V Afanas'ev, N. G. Basov, O. N. Krokhin, V. V. Pustovalov, V. P. Silin, G. V. Sklizkov, V. T. Tikhonchuk, and A. S. Shikanov, Vzaimodeĭstvie moshchnogo lazernogo izlucheniya s plazmoĭ (Interaction of Intense Laser Radiation with Plasma), VINITI, 17 (1978).
[2]M. D. Rosen, D. W. Phillion, V. C. Rupert, W. C. Mead, W. L. Kruer, J. J. Thomson, H. N. Kornblum, V. W. Slivinsky, G. J. Caporaso, M. J. Boyle and K. G. Tirsell, Phys. Fluids 22, 2020 (1979).
[3]P. G. Burkhalter, F. C. Young, B. H. Ripin, N. M. McMahon, S. E. Bodner, R. R. Whitlock, and D. J. Nagel, Phys. Rev. A15, 1191 (1977).
[4]V. V. Aleksandrov, S. I. Anisimov, M. V. Brenner, E. P. Velikhov. V. D. Vikharev, V. P. Zotov, N. G. Koval'skiĭ, M. I. Pergament, and A. I. Yaroslavskiĭ, Zh. Eksp. Teor. Fiz. 71, 1826 (1976) [Sov. Phys. JETP 44, 958 (1976)].
[5]D. M. Villeneuve, G. D. Enright, M. C. Richardson, and N. R. Isenor, J. Appl. Phys. 50, 3921 (1979).
[6]V. V. Blazhenkov, A. N. Kirkin, L. P. Kotenko, A. M. Leontovich, G. I. Merzon, A. M. Mozharovskiĭ, A. L. Cher-

nyakov, and A. N. Chuzo, Zh. Eksp. Teor. Fiz. **78**, 1386 (1980) [Sov. Phys. JETP **51**, 697 (1980)].
[7]Yu. A. Zakharchenkov, O. N. Krokhin, G. V. Sklizkov and A. S. Shikanov, Kvant. Elektron. (Moscow) **3**, 1068 (1976) [Sov. J. Quantum Electron. **6**, 571 (1976)].
[8]L. M. Gorbunov, Yu. S. Kas'yanov, V. V. Korobkin, A. N. Plyanichev, and A. P. Shevel'ko, FIAN Preprint No. 126, 1979.
[9]L. M. Gorbunov, Yu. S. Kas'yanov, V. V. Korobkin, A. N. Polyanichev, and A. P. Shevel'ko, Pis'ma Zh. Eksp. Teor. Fiz. **27**, 242 (1978) [JETP Lett. **27**, 226 (1978)].
[10]J. W. Shearer, S. W. Mead, J. Petruzzi, F. Rainer, I. E. Swain, and C. E. Violet, Phys. Rev. **A6**, 764 (1972).
[11]P. Kolodner and E. Yablonovitch, Phys. Rev. Lett. **37**, 1754 (1976).
[12]A. N. Kirkin, A. M. Leontovich, and A. M. Mozharovskiĭ, Kvant. Elektron. (Moscow) **5**, 2640 (1978) [Sov. J. Quantum Electron. **8**, 1489 (1978)].
[13]V. V. Blazhenkov, S. F. Kozlov, L. P. Kotenko, G. I. Merzon, and A. N. Chuzo, FIAN Preprint No. 202 (1977).
[14]AD811 and QD808 Operating and Service Manual, EG&G/ ORTEC, Midland Road, Oak Ridge TN 37830.
[15]O. N. Krokhin, Yu. A. Mikhaĭlov, V. V. Pustovalov, A. A. Rupasov, A. A. Rupasov, V. P. Silin, G. V. Sklizkov, and A. S. Shikanov, Zh. Eksp. Teor. Fiz. **69**, 206 (1975) [Sov. Phys. JETP **42**, 107 (1975)].
[16]B. H. Ripin and E. A. McLean, Appl. Phys. Lett. **34**, 809 (1979).
[17]A. G. M. Maaswinkel, K. Eidmann, and R. Sigel, Phys. Rev. Lett. **42**, 1625 (1975).
[18]A. G. M. Maaswinkel, Optics Commu. **33**, 62 (1980).
[19]O. T. Baĭkov, A. A. Mak, R. N. Medvedev, V. A. Serbryakov, and N. A. Solov'ev, Pis'ma Zh. Eksp. Teor. Fiz. **29**, 44 (1979) [JETP Lett. **29**, 40 (1979)].
[20]D. M. Woodall, B. Yaakobi, and M. J. Lubin, Laser Induc. Fus. and X-ray Laser Stud., Reading, Mass, 1976, p. 191.
[21]A. N. Kirkin, A. M. Leontovich, A. M. Mozharovskiĭ, and E. N. Ragozin, Kvant. Elektron. (Moscow) **6**, 2251 (1979) [Sov. J. Quantum Electron. **9**, 1322 (1979)].
[22]F. C. Yahoda, E. M. Little, W. E. Quinn, G.A. Sawyer, and T. F. Stratton, Phys. Rev. **119**, 843 (1960).
[23]A. I. Tikhonov and V. Ya. Arsenin, Metody resheniya nekorrektnykh zadach (Methods of Solving Incorrect Problems), Nauka, 1979.
[24]P. A. Ross, J. Opt. Soc. Am. **16**, 433 (1928).
[25]V. V. Slivinsky and H. N. Kornblum, Bull. Am. Phys. Soc. **18**, 1256 (1973).
[26]H. D. Shay, R. A. Haas, W. L. Kruer, M. J. Boyle, D. W. Phillion, V. C. Rupert, H. N. Kornblum, F. Rainer, V. W. Slivinsky, L. N. Koppel, L. Richards, and K. G. Tirsell, Phys. Fluids **21**, 1643 (1978).
[27]B. H. Ripin, F. C. Young, J. A. Steamper, C. M. Armstrong, R. Decoste, E. A. McLean, and S. E. Bodner, Phys. Rev. Lett. **39**, 611 (1977).
[28]V. V. Blazhenkov, A. N. Kirkin, A. M. Leontovich, A. M. Mozharovskiĭ, and A. N. Chuzo, Pis'ma Zh. Tekh. Fiz. **4**, 945 (1978) [Sov. Tech. Phys. Lett. **4**, 380 (1978)].
[29]D. W. Forslund, J. M. Kindel, and K. Lee, Phys. Rev. Lett. **39**, 284 (1977).
[30]Tai Ho Tan, A. H. Williams, and G. H. McCall,(1979) IEEE Int. Conf. on Plasma Science, Montreal, Canada, 1979.
[31]K. R. Manes, H. G. Ahlstom, R. A. Haas, J. F. Holzrichter, J. Opt. Soc. Am. **67**, 717 (1977).
[32]B. Luther-Davies, Opt. Commun. **23**, 98 (1977).
[33]F. C. Young, S. P. Obenschain, and B. H. Ripin,(1979) IEEE Int. Conf. on Plasma Science, Montreal, Canada, (1979).
[34]V. V. Aleksandrov, V. D. Vikharev, V. V. Gavrilov, Yy. S. Petrykin, A. V. Sennik, and A. I. Yaroslavskii, IAÉ Preprint No. 3158, 1979.
[35]K. Eidmann, Plasma Phys. **17**, 121 (1975).
[36]O. N. Krokhin, Yu. A. Mikhaĭlov, V. V. Pustovalov, A. A. Rupasov, V. P. Silin, G. V. Sklizkov, and A. S. Shikanov, Pis'ma Zh. Eksp. Teor. Fiz. **20**, 239 (1974) [JETP Lett. **20**, 105 (1974)].
[37]R. P. Godwin, J. F. Kephart, and G. H. McCall, Bull. Amer. Phys. Soc. **17**, 971 (1972).
[38]J. L. Shohet, D. B. Van Hulsteyn, S. J. Gitomer, J. F. Kephart, R. P. Godwin, Phys. Rev. Lett. **38**, 1024, 1977.
[39]V. V. Blazhenkov, S. D. Zakharov, A. N. Kirkin, A. V. Kononov, L. P. Kotenko, A. M. Leontovich, G. I. Merzon, and A. M. Mozharovskiĭ, Pis'ma Zh. Eksp. Teor. Fiz. **31**, 352 (1980) [JETP Lett. **31**, 321 (1980)].
[40]P. Kirkpatrick and L. Widmann, Phys. Rev. **67**, 321 (1945).
[41]K. Estabrook, E. Valeo, and W. L. Kruer, Phys. Fluids **18**, 1151 (1975).
[42]J. S. Pearlman and M. K. Matzen, Phys. Rev. Lett. **39**, 140 (1977).
[43]B. Luther-Davies, Appl. Phys. Lett. **32**, 209 (1978).
[44]D. W. Forslund, J. M. Kindel, K. Lee, and E. L. Lindman, Proc. Indian Acad. Sci. **86A**, 193 (1977).

Translated by J. G. Adashko